AD_____

Award Number: W81XWH-10-2-0048

TITLE: Discovery and Testing of Ricin Therapeutics

PRINCIPAL INVESTIGATOR: Domenico Tortorella, Ph.D.

CONTRACTING ORGANIZATION: Mount Sinai School of Medicine
New York, NY 10029

REPORT DATE: June 2012

TYPE OF REPORT: Final

PREPARED FOR: U.S. Army Medical Research and Materiel Command
Fort Detrick, Maryland 21702-5012

DISTRIBUTION STATEMENT: Approved for Public Release;
Distribution Unlimited

REPORT DOCUMENTATION PAGE

Form Approved
OMB No. 0704-0188

1. REPORT DATE	2. REPORT TYPE	3. DATES COVERED
June 2012	Final	17 May 2010 – 16 May 2012

4. TITLE AND SUBTITLE

Discovery and Testing of Ricin Therapeutics

5a. CONTRACT NUMBER

5b. GRANT NUMBER
W81XWH-10-2-0048

5c. PROGRAM ELEMENT NUMBER

6. AUTHOR(S)

Domenico Tortorella
Veronika Redmann

E-Mail: domenico.tortorella@mssm.edu

5d. PROJECT NUMBER

5e. TASK NUMBER

5f. WORK UNIT NUMBER

7. PERFORMING ORGANIZATION NAME(S) AND ADDRESS(ES)

Mount Sinai School of Medicine
New York, NY 10029

8. PERFORMING ORGANIZATION REPORT NUMBER

9. SPONSORING / MONITORING AGENCY NAME(S) AND ADDRESS(ES)
U.S. Army Medical Research and Materiel Command
Fort Detrick, Maryland 21702-5012

10. SPONSOR/MONITOR'S ACRONYM(S)

11. SPONSOR/MONITOR'S REPORT NUMBER(S)

12. DISTRIBUTION / AVAILABILITY STATEMENT
Approved for Public Release; Distribution Unlimited

13. SUPPLEMENTARY NOTES

14. ABSTRACT

Ricin is an extremely potent A-B toxin that is transported from the cell surface to the cytosol where it inactivates ribosomes leading to cell death. Ricin access to the cytosol is dependent on its transport from the cell surface to the ER lumen. We have established a ricin A chain dislocation assay using enzymatic attenuated ricin A chain molecules (RTAE177D and RTAdelta). The ricin A chains undergoes a rapid transport across the ER membrane and is eventually degraded by the proteasome. The instability of ricin A chain was developed into a high-throughput screen to identify chemicals that block ricin transport. A green fluorescent protein (GFP) ricin chimera was created to screen chemical libraries in ricin dislocation inhibitors. Using a high-content screen, we have screened a small bioactive 'FDA'-approved chemical library consisting of 2080 compounds and >35,000 compounds from a large chemical library referred to as L1. Presently, we have identified at least eight diverse family of compounds that increased the stability of the ricin-GFP chimera. Secondary assays have confirmed the stability of ricin and other cellular degradation substrates. The data demonstrate that these chemicals could be used to block ricin and may be effective against other pathogens and human diseases.

15. SUBJECT TERMS
Ricin toxin, dislocation, small weight compounds, chemical inhibitors, high-content screen, fluorescent-based cell assay

16. SECURITY CLASSIFICATION OF:			17. LIMITATION OF ABSTRACT	18. NUMBER OF PAGES	19a. NAME OF RESPONSIBLE PERSON
a. REPORT	b. ABSTRACT	c. THIS PAGE			USAMRMC
U	U	U	UU	13	19b. TELEPHONE NUMBER *(include area code)*

Table of Contents

Page

INTRODUCTION:

Ricin is derived from *Ricinus communis* and is classified as a select agent by the U.S. Departments of Health and Human Services (HHS) and Centers for Disease Control and Prevention (CDC). The toxin's ability to kill cells and the potential to make large quantities of the toxin using low-tech strategies can be exploited by terrorist organizations or individuals to develop ricin into a biological weapon. Strikingly, ricin toxin was manufactured and stored as a biological weapon by Iraq (18) and numerous cases of potential exposure were documented in London, UK (14), France (24), Washington DC, (31) and Georgia, US (22). Therefore, ricin exposure is a real threat to the general population as well as military personnel, but there are very limited therapies to treat individuals exposed to the toxin.

Ricin toxin is a member of the A-B family of toxins, which also includes cholera toxin, diphtheria toxin, shiga toxin, *Pseudomonas* exotoxin A and pertussis toxin (25). Ricin toxin enters the cell through endocytosis following interaction of the B subunit with cell surface glycolipids and glycoproteins. It then traffics in a retrograde fashion through the trans-Golgi network and Golgi apparatus towards the ER, eventually acting on the ribosome in the cytoplasm (13). Ricin toxin is a type-II ribosome inactivating protein, or RIP. Type II RIPs act upon the ribosome by depurinating an adenine residue in the region of the 28S rRNA termed the sarcin-ricin loop, thereby halting translation and inducing cell death (4).

The retrograde transport of the ricin A chain across the ER membrane and into the cytosol known as dislocation utilizes the cellular process referred to as ER quality control. The ER environment mediates the folding of nascent polypeptides into their native conformations. Proteins that cannot adopt a proper folded conformation due to deleterious effects of folding or genetic mutations may be extracted from the ER and transported to the cytosol for proteasome degradation (7, 17, 21). There is a growing list of human diseases that can be attributed to the destruction of proteins from the ER (**Table 1**) (2, 3). Thus, ricin utilizes a cellular pathway designated to eliminate misfolded ER proteins in order to gain access to the cytosol.

Table 1. Some diseases associated with degradation from the ER

Disease	Defective gene/proteins	Clinical Manifestation	Cellular pathology
Cystic fibrosis	cystic fibrosis transmembrane conductance regulator (CFTR)	lung disease	ER retention and degradation
Emphysema	α_1-antitrypsin variants	lung disease	ER degradation
Fabri disease	α -D-galactosidase	neurological disease	ER degradation
Oculocutaneous albinism	tyrosinase	pigmentation defect	ER retention and degradation
Diabetes mellitus	insulin receptor	diabetes	ER retention and degradation
Protein C deficiency	Protein C	blood disease	ER retention and degradation

The investigation of ricin toxin transport across the ER membrane has been hampered by the low number of toxin molecules that reach the ER lumen when added extracellularly (28). In order to study how ricin A chains (RTA) are dislocated across the bilayer in human cells, we established a human cell system in which the ricin A chain was ectopically expressed in the ER (23). However, due to the toxic nature of wild type RTA upon expression in human cells, we generated a ricin A chain point mutant (RTA_{E177D}) (23) that is structurally similar to wild type (1), but enzymatically attenuated (6, 26). This mutant was stably expressed in a human astrocytoma cell line (U373) ($U373^{RTAE177D}$) because these cells are sensitive to ricin and support dislocation of ER substrates (5, 15, 16, 19, 29, 30). Our data supports a model that ricin A chain dislocation occurs via a novel strategy by utilizing the hydrophobic nature of the ER membrane and selective ER components (e.g. SEL1L (suppressor of lin-12-like), and not Derlin-1) (23). The ERAD components EDEM-1, HRD E3-ligase, Png-1, Rad23 proteasome receptor, and Yos9 were found to be important for ricin dislocation (9, 11, 12, 27), while other factors such as ubiquitin and Derlin-1 are indispensible for ricin dislocation confirming our findings that ricin co-opts specific components of ERAD (12). A striking result from our studies was that the ricin A chain was dislocated across the ER membrane with fast kinetics and eventually degraded by the proteasome. Thus, we utilized the fast kinetics of dislocation as the basis for a high-throughput assay to discover compounds that stabilize ricin A chain in the ER.

BODY:

Generation of RTA_{E177D}-GFP expressing cells: In order to develop a high throughput assay to identify compounds that stabilize ricin A chain, we constructed a ricin chimera consisting of an N-terminal K^b signal peptide, the enzymatically attenuated RTA_{E177D}, and a carboxy-terminus enhanced green fluorescent protein (GFP) (RTA_{E177D}-GFP) (**Fig. 1A**). This construct was retrovirally transduced into human U373 astrocytoma cells (20) to create cells expressing RTA_{E177D}-GFP ($U373^{RTAE177D\text{-}GFP}$). The protein levels of RTA_{E177D}-GFP were stabilized upon inclusion of proteasome inhibitor carboxybenzyl-leucyl-leucyl-leucyl vinyl sulfone (ZL_3VS) (**Fig. 1B**). This result was consistent with published data using a non-GFP version of ricin (RTA_{E177D}) (23). The consistent accumulation of the glycosylated RTA_{E177D}-GFP proteins (**Fig. 1B, lanes 3 & 5**) in two clones (3 and 4) indicated that the RTA chimera was stabilized in the ER. These data demonstrate that U373 cells that express the RTA-GFP chimera fulfill an important criterion for the establishment of a high-throughput screen.

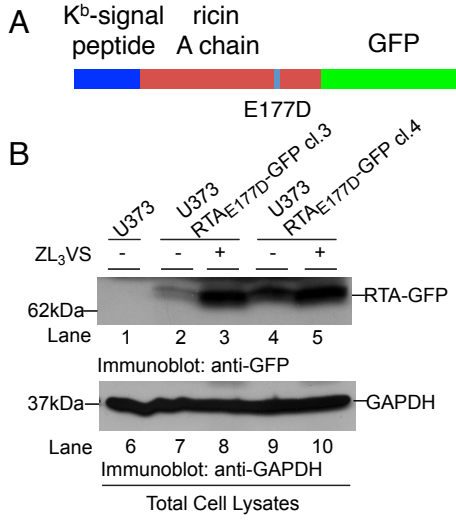

Figure 1. RTA_{E177D}-GFP was stabilized upon proteasome inhibition. U373 cells expressing RTA_{E177D}-GFP (**A**) (clones 3 and 4) were untreated and treated with proteasome inhibitor (ZL_3VS) (2.5μM and 14hrs) and analyzed by immunoblot analysis (**B,** lanes 1-5). A glyceraldehyde 3-phosphate dehydrogenase (GAPDH) immunoblot confirmed equivalent protein loading (**B**, lanes 6-10). Polypeptides and molecular weight markers are indicated.

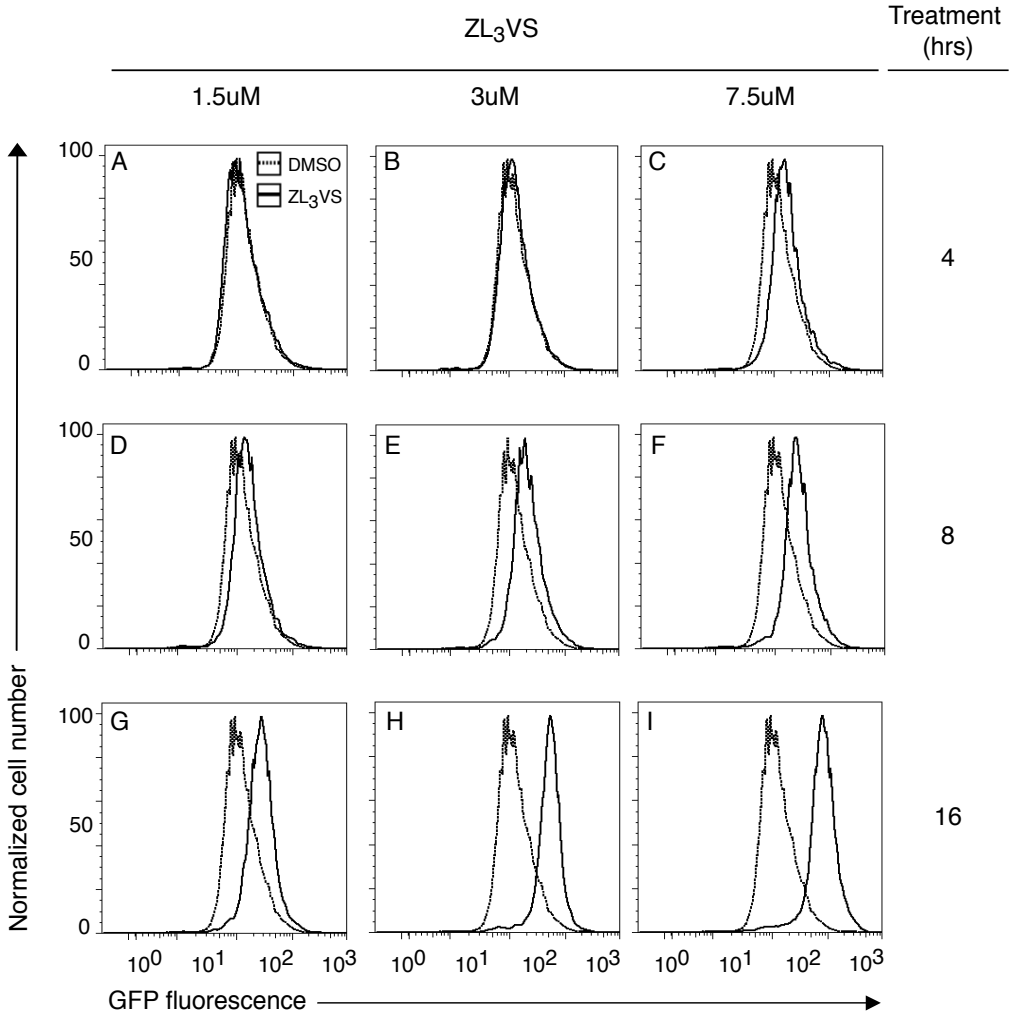

Establishing conditions for stabilizing ricin A chain: We next optimized proteasome inhibition conditions to visualize the stabilization of K_b-RTA_{E177D}-GFP molecules. U373 cells expressing K_b-RTA_{E177D}-GFP were treated for 4, 8 or 16 hours and with 1.5, 3 or 7.5uM ZL_3VS and then evaluated by flow cytometry (**Fig. 2**). The data demonstrated that a lower concentration of ZL_3VS (1.5 μM) required 16hrs to observe a significant increase in GFP fluorescence (**Fig. 2. A, D, and G**). However, incubation of 7.5 μM of ZL_3VS for only 8 hours revealed a measurable increase in GFP

Figure 2. Analysis of RTA-GFP stabilization by flow cytometry. U373$^{RTAE177D-GFP}$ cells (clone 4) treated with different concentrations of proteasome inhibitor (ZL_3VS) (1.5μM (A,D,G), 3μM (B,E,H), or 7.5μM (C,F,I)) for 4hrs (A-C), 8 hrs (D-F), or 16 hrs (G-I) were analyzed for GFP fluorescence using a Beckman Coulter Cytomics FC 500 Flow Cytometer. The results were plotted as normalized cell number versus GFP fluorescence comparing DMSO (dashed line) or ZL_3VS (solid line) treated cells.

fluorescence with even a higher GFP signal following a 16 hour incubation (**Fig. 2. C, F, and I**). Cells treated with 3 μM of ZL_3VS also induced a robust increase in GFP fluorescence following a 16 hour incubation (**Fig. 2. B, E, and H**). Considering cell morphology as an indication of cell health, the optimal treatment time and concentration for ZL_3VS treatment was determined as 3μM for 16 hours. Together, these results provided the proof-of-concept that U373$^{RTAE177D-GFP}$ cells could be utilized in a high-throughput assay to discover compounds that stabilize RTA.

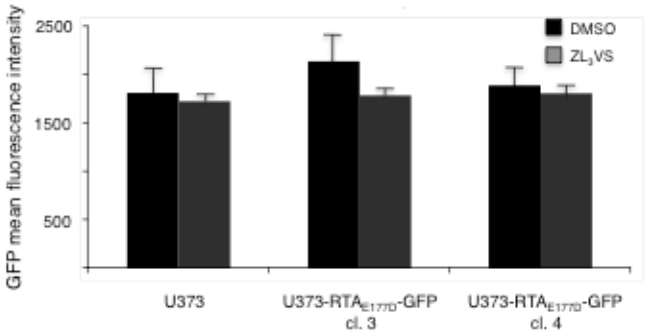

Figure 3. Analysis of RTA-GFP stabilization by fluorescence palte reader. U373 cells and U373$^{RTAE177D-GFP}$ cells (clones 3 and 4) were plated into a 384 well plate (7,500 cells/well) untreated (black bars) or proteasome inhibitor (ZL_3VS) treated (gray bars) (3 μM, 16 hrs). The GFP mean fluorescence intensity was averaged from the three wells and the difference among the signal was represented by the error bars.

Establish conditions to utilize U373$^{RTAE177D-GFP}$ cells in a high-content screen: Our initial experiment measured the overall fluorescence signal of U373$^{RTAE177D-GFP}$ cells treated with proteasome inhibitor ZL_3VS in a 384 well plate (**Fig. 3**). Clones 3 and 4 of U373$^{RTAE177D-GFP}$ cells (in triplicate) were untreated or treated with ZL_3VS (3μM, 16 hrs), washed twice with PBS followed by the measurement of GFP fluorescence using a Perkin Elmer EnVision plate reader housed within the MSSM Experimental Therapeutics Institute Integrated Screening Core (ETI-ISC). Two clones were utilized to validate any findings. Only a small increase in fluorescent signal was observed from U373$^{RTAE177D-GFP}$ cells treated with proteasome inhibitor (**Fig. 3**); thus, this strategy of analysis could not be used in a high-throughput screen.

Thus, we analyzed proteasome inhibitor-treated U373$^{RTAE177D-GFP}$ cells by a more sensitive method utilizing the Molecular Devices ImageXpress Ultra (IXU) plate-scanning confocal microscope designed for high-throughput analysis at the ETI-ISC. U373$^{RTAE177D-GFP}$ cells treated with proteasome exclusively demonstrated a measurable punctate pattern of GFP fluorescent signal (**Fig. 4**). Four fields/well were acquired by the IXU confocal microscope and MetaExpress software was used to quantify the fluorescent signal from U373$^{RTAE177D-GFP}$ cells. Each image was analyzed based on the nuclear stain (**Fig. 4,** (blue, 4',6-diamidino-2-phenylindole (DAPI) stain) and a GFP fluorescent signal. A mask was created to identify the nucleus ranging from 7-30μm and 1500 gray levels over background, while the RTA$_{E177D}$-GFP proteins were detected by analyzing GFP fluorescent granules between 2-4μm and 3000 gray levels above background. The GFP fluorescent signal was calculated into an integrated granule intensity/total granule area of the cell and these values were used to

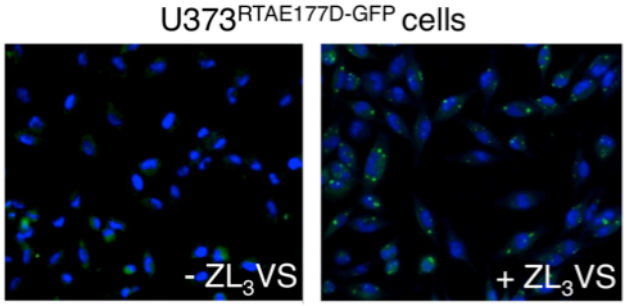

Figure 4. Proteasome inhibition induces fluorescent granules in proteasome treated U373$^{RTAE177D-GFP}$ cells. U373$^{RTAE177D-GFP}$ cells treated with or without proteasome inhibitor (ZL_3VS, 2.5 μM) for 16hrs were subjected to fluorescence confocal microscopy. The nucleus (DAPI, blue) and RTA$^{E177D-GFP}$ (green fluorescent granules) molecules were analyzed.

determine the assay fitness parameter known as the Z' factor value. The Z' factor ($Z'=1-[3s_{C+} + 3s_{C-}]/[m_{C+} - m_{C-}]$) is calculated from the standard deviations of the positive and negative control data sets ($s_{C+} + 3s_{C-}$) and mean values of the positive and negative controls ($m_{C+} - m_{C-}$). We optimized the experimental conditions to generate a consistent and robust Z' factor value by modifying cell number/well, proteasome inhibitor concentration, and incubation time of proteasome inhibitor (**Table 2**). In addition, the coefficient of variation (CV) of the Z' factor was determined by analyzing different plates the same day and day-to-day variation. In general, $U373^{RTAE177D-GFP}$ cells yielded a great Z' factor value with a low CV value validating the fitness of the high-content screen.

Table 2: Optimized conditions for RTA high-content screen

Conditions	Values
Average Z' factor value (6 experiments)	0.74 +/-0.04
Analysis time post proteasome inhibitor	14 hrs
Proteasome inhibitor concentration	2.8μM
Cell number	3000
Tolerable DMSO concentration	1.5%
Coefficient of variability	4.5%

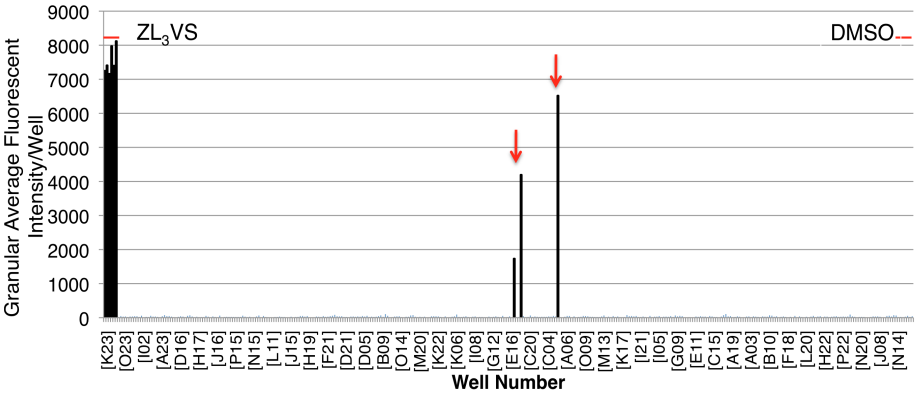

Figure 5. Analysis of high-content screen from $U373^{RTAE177D-GFP}$ cells treated with FDA approved drugs. The figure represents the data recovered from $U373^{RTAE177D-GFP}$ treated with 320 FDA-approved drugs, DMSO (negative controls), and ZL_3VS (2.8μM, positive controls). The red arrows represent hit compounds that stabilize $RTA^{E177D-GFP}$.

High-content screening of the bioactive 'FDA-approved' compound library: Utilizing the optimized screening conditions, we screened the bioactive 'FDA-approved' chemical compound library consisting of 2,080 compounds in triplicate available at the ETI-ISC. In general, $U373^{RTAE177D-GFP}$ cells were plated in a 384 well plate (3,000 cells/well, 30 μl). The respective compounds were then pinned (20nl, ~5μM final) in each well and incubated at 37°C for 14 hrs. The cells were then washed twice with PBS and fixed with 4% paraformaldehyde. Six positive (ZL_3VS, 2.8μM) and negative (DMSO-treated) controls were included in each plate. The granular average intensity/well was determined as described above and a typical result from a 384 well plate is shown in **Figure 5**. We considered a compound a hit when the average granular intensity is >50% of the GFP intensity compared to proteasome inhibitor treated $U373^{RTAE177D-GFP}$ cells and a >0.60 Z' factor. In the case of **Figure 5**, the Z' factor value would only be calculated from wells whose compound yielded an intensity >3750 (50% of ~7500 average granular intensity of ZL_3VS treated cells). These wells would be visually inspected to confirm the increase in GFP fluorescent perinuclear granules (**Fig. 4**). Using these criteria, eleven hit compounds were identified from the screening of the bioactive 'FDA-approved' compound library (**Table 3**). Strikingly, two sets of compounds have similar chemical structures (* and **) suggesting that these compounds may be effective at stabilizing RTA. The hit compounds

Table 3: Hit compounds from bioactive 'FDA-approved' chemical library

Chemical name
Acetyl Isogambogic Acid**
Acriflavinium hydrochloride
Anthothecol
1-Benzylcarbonylaminophenethlchloromethylyketone
Celastrol*
Dihydrocelastryl Diacetate*
Dihydrogambogic Acid**
Gambogic Acid Amide**
Gentian Violet
Merbromin
Tetrachloroisophthalonitrile
** and ** indicate structurally similar compounds*

were purchased for secondary assays excluding gambogic acid amide and dihydrogambogic acid because they were unavailable from commercial sources.

Analysis of hit compounds from bioactive 'FDA-approved' chemical library.

Our initial secondary assay examined the ability of the hit compounds to stabilize RTA_{E177D} molecules lacking the GFP protein. $U373^{RTAE177D}$ cells treated with 2.5, 5, and 10 μM of the respective hit compounds or proteosome inhibitor ZL_3VS (2.5 μM) for 16 hrs were subjected to an immunoblot analysis for RTA and glyceraldehyde 3-phosphate dehydrogenase (GAPDH) (**Fig. 6**). As expected, the cells treated with proteosome inhibitor caused the stabilization of both the glycosylated (+CHO) and deglycosylated (-CHO) RTA molecules (**Fig. 6, A, B, C, and D, lane 3**) (23). The observation of the deglycosylated version of the RTA indicates that the polypeptide has been dislocated across the membrane exposing part of the protein to the cytosol. Examination of the total RTA protein levels from cells treated with the hit compounds demonstrated that anthothecol, acetyl isogambogic acid, gentian violet, celestrol, dihydrocelastryl diacetate, and tetrachloroisophthalonitrile induced a robust stabilization of RTA molecules (**Fig. 6A-D**). Also, 1-benzylcarbonylaminophenethlchloromethylyketone only slightly increased the levels of RTA (**Fig. 6D, lanes 4-6**). In contrast, merbromin and acriflavinium hydrochloride were ineffective at stabilizing ricin A chain molecules (**Fig. 6B**). The GAPDH immunoblot demonstrated equivalent protein loading (**Fig. 6, A, C, and D (lanes 10-18) and B (lanes 13-24)**). The hit compounds gentian violet, celestrol, and dihydrocelastryl diacetate stabilized a higher proportion of the glycosylated RTA species suggesting that they may target a step prior to dislocation. On the other hand, anthothecol, acetyl isogambogic acid, and tetrachloroisophthalonitrile stabilized both forms of RTA at equivalent levels suggesting that a step downstream of dislocation was probably altered by the compound (**Fig. 6A and C**). Collectively, these compounds displayed a varied effect on RTA stability and may be potential reagents that can prevent ricin intoxication.

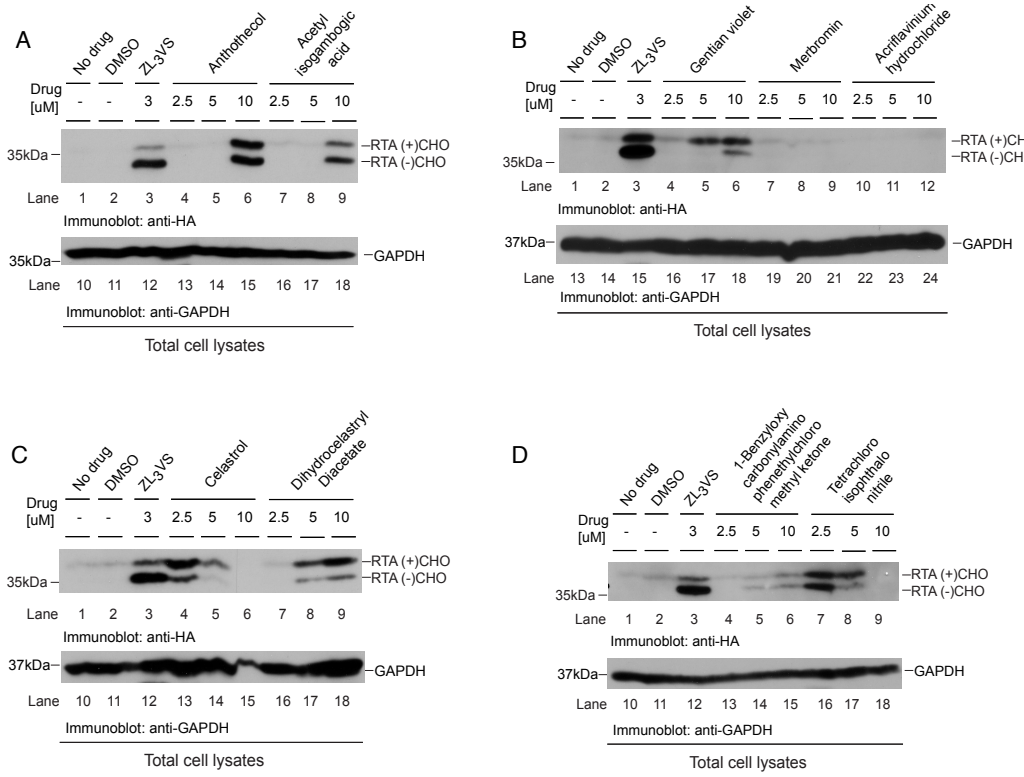

We next examined whether the most effective hit compounds that stabilize ricin A chain would also increase the levels of a classical ER degradation substrate. The stabilization of an ER degradation substrate would indicate that the compound may be effective against genetic

Figure 6. Analysis of hit compounds that stabilize RTA_{E177D} species. Total cell lysates from U373 K_b-RTA_{E177D} cells treated with DMSO, ZL_3VS or hit compounds (A-D) were subjected to immunoblot analysis for RTA (A, B, and D, lanes 1-9 and B, lanes 1-12) and GAPDH (A, B, and D, lanes 10-18 and B, lanes 13-24)). The respective polypeptides and molecular weight markers are indicated.

diseases that are due to misfolded ER polypeptides (**Table 1**). Thus, we examined the levels of TCRα chain because it is a well-characterized ER dislocation substrate that is degraded with fast kinetics (8, 10). U373 cells expressing TCRα chain were untreated or treated with ZL_3VS or the respective hit compounds and analyzed by immunoblot analysis (**Fig. 7**). Typically, TCR α chain is degraded in a proteasome dependent manner as observed by the increased stability of both glycosylated (+CHO) and deglycosylated (-CHO) TCR α chain upon ZL_3VS treatment (**Fig. 7, lanes 2-4**). Strikingly, anthothecol, dihydrocelastryl acetate, celestrol, and acetyl isogambogic acid induced a significant increase in levels of TCR α chain (**Fig. 7, lanes 5-11**). These compounds mostly induced the accumulation of glycosylated TCR α chain species indicating they have attenuated the dislocation reaction. Gentian violet, tetrachloroisophthalonitrile, and 1-benzylcarbonylaminophenethlchloromethylyketone only marginally induced an increase in levels of the TCR α chain species (**Fig. 7, lanes 5, 10, and 11**). Note, gentian violet treated cells induced a small increase in TCR α chain and higher-molecular weight species likely due to ubiquitinylation (**Fig. 7, lane 5 and data not shown**). The calnexin immunoblot demonstrated equivalent protein loading (**Fig. 7, lanes 12-22**). The data suggest that gentian violet and tetrachloroisophthalonitrile may be specific for stabilizing ricin A chain, while anthothecol, dihydrocelastryl acetate, celestrol, and isogambogic acid likely target a protein or pathway that is common for the destabilization of ricin A chain and a misfolded ER protein. Collectively, these results imply that ricin specific compounds could be identified utilizing our high-content screen as well as compounds that may be effective against other ER substrates.

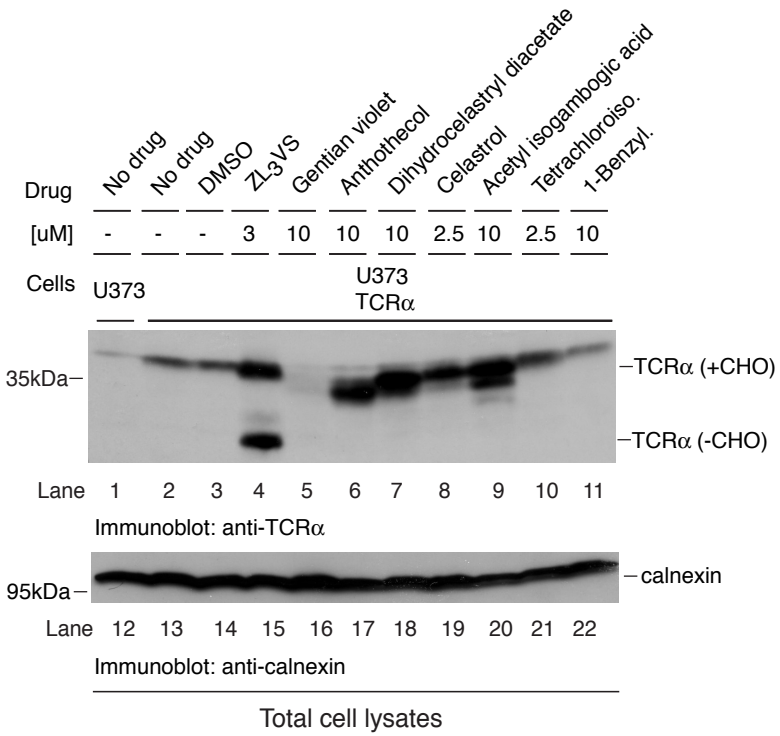

Figure 7. Analysis of hit compounds that stabilize TCRα chain. Total cell lysates from U373 and U373 TCRα cells treated with DMSO, ZL_3VS or hit compounds at the indicated concentration for 14hrs were subjected to immunoblot analysis for TCRα chains (lanes 1-11) and calnexin (lanes 12-22). The respective polypeptides and molecular weight markers are indicated

High-content screening of L1 library.

We next began screening the L1 library that is comprised of 100,000 compounds selected from the Chembridge library collection targeting membrane and cellular pathways at the MSSM ETI-ISC. We have screened over 35,000 compounds and eight compounds were identified as hit compounds (**Table 4**). These compounds represent reagents that provided a >0.9 Z' factor indicating they induced

Table 4: Hit compounds from currently screened L1 library
Chemical name
2-[(3-methyl-4-nitrobenzoyl)amino]-4,5,6,7,8,9-hexahydrocycloocta[b]thiophene-3-carboxamide
2-(3-methoxyphenyl)-6-(1-piperidinyl)-1H-benzo[de]isoquinoline-1,3(2H)-dione
3-(benzylamino)benzo[b]-1,6-naphthyridine-4-carbonitrile
5-bromo-N-[3-(5-chloro-1,3-benzoxazol-2-yl)-2-methylphenyl]nicotinamide
N-ethyl-N-{2-[(5-nitro-8-quinolinyl)amino]ethyl}benzenesulfonamide
4-[5-(4-bromophenyl)-4,7-dihydrotetrazolo[1,5-a]pyrimidin-7-yl]-N,N-dimethylaniline
2-(4-bromo-2-methylphenoxy)-N-(4-methoxy-2-nitrophenyl)acetamide

consistent GFP emitting granules. Secondary assays will be performed to determine whether these compounds specifically stabilize ricin A chain or are general inhibitors of the dislocation and degradation processes for misfolded ER proteins.

KEY RESEARCH ACCOMPLISHMENTS:

- Isolated single clones of human U373 cells that express the RTA_{E177D}-GFP chimera.
- Optimized proteasome inhibitor ZL_3VS treatment of $U373^{RTAE177D\text{-}GFP}$ cells for the high content-screen.
- Screened bioactive 'FDA-approved' chemical library of 2080 compounds.
- Screened >35,000 compounds from the L1 chemical library at the Mount Sinai School of Medicine Experimental Therapeutic Institute.
- Eleven hit compounds were identified from the bioactive 'FDA-approved' chemical library that stabilized RTA_{E177D}-GFP.
- Six hit compounds from the bioactive 'FDA-approved' chemical library stabilized RTA_{E177D} molecules using an immunoblot assays.
- Four hit compounds from the bioactive 'FDA-approved' chemical library stabilized the ER dislocation substrate TCR α chain.
- Two compounds from the bioactive 'FDA-approved' chemical library may specifically stabilize RTA_{E177D}.
- Eight hit compounds from ~35,000 compounds of the L1 library were identified as hit compounds that stabilized RTA_{E177D}-GFP.

REPORTABLE OUTCOMES:

Manuscripts:

1) Redmann, V., Lau, W., Morohashi, K., Felsenfeld, D., and Tortorella, D. (2012) Identification of novel compounds that stabilize ricin A chain utilizing granularity parameters in a high through-put screen, *in preparation*.
2) Redmann, V. and Tortorella, D. (2012) Characterization of novel compounds that stabilize ricin A chain in the ER, *in preparation*.

Compounds identified to stabilize ricin A chain:

Chemical name	Chemical Library
Acetyl Isogambogic Acid	Bioactive 'FDA-approved' library
Acriflavinium hydrochloride	Bioactive 'FDA-approved' library
Anthothecol	Bioactive 'FDA-approved' library
1-Benzylcarbonylaminophenethlchloromethylyketone	Bioactive 'FDA-approved' library
Celastrol	Bioactive 'FDA-approved' library
Dihydrocelastryl Diacetate	Bioactive 'FDA-approved' library
Dihydrogambogic Acid	Bioactive 'FDA-approved' library
Gambogic Acid Amide	Bioactive 'FDA-approved' library
Gentian Violet	Bioactive 'FDA-approved' library
Merbromin	Bioactive 'FDA-approved' library
Tetrachloroisophthalonitrile	Bioactive 'FDA-approved' library
2-[(3-methyl-4-nitrobenzoyl)amino]-4,5,6,7,8,9-hexahydrocycloocta[b]thiophene-3-carboxamide	L1 library
2-(3-methoxyphenyl)-6-(1-piperidinyl)-1H-benzo[de]isoquinoline-1,3(2H)-dione	L1 library
3-(benzylamino)benzo[b]-1,6-naphthyridine-4-carbonitrile	L1 library
5-bromo-N-[3-(5-chloro-1,3-benzoxazol-2-yl)-2-methylphenyl]nicotinamide	L1 library
N-ethyl-N-{2-[(5-nitro-8-quinolinyl)amino]ethyl}benzenesulfonamide	L1 library
4-[5-(4-bromophenyl)-4,7-dihydrotetrazolo[1,5-a]pyrimidin-7-yl]-N,N-dimethylaniline	L1 library
2-(4-bromo-2-methylphenoxy)-N-(4-methoxy-2-nitrophenyl)acetamide	L1 library

CONCLUSION:

We have established a human cell-based strategy to discover anti-ricin therapeutics. U373 cells that express the RTA_{E177D}-GFP chimera were utilized in a high-content screen to identify compounds that stabilize the RTA_{E177D}-GFP molecule within the ER compartment. The accumulation of RTA_{E177D}-GFP proteins in the ER suggests that the polypeptide is unable to access the cytosol and intoxicate cells. We have performed a high-content screen at MSSM Experimental Therapeutics Institute Integrated Screening Core which is well equipped with a full-time screening staff, state-of-the-art high-throughput technology, and technical expertise. To date, we have screened a bioactive 'FDA-approved' chemical library (2080 compounds) and part of a L1 chemical library (>35,000) at the MSSM Screening Core. We have identified 19 compounds that stabilize RTA_{E177D}-GFP with 11 compounds from the bioactive 'FDA-approved' chemical library (**Table 3**) and 8 from the L1 library (**Table 4**). Of the identified 19 compounds, 11 compounds were subjected to secondary assays to validate the effectiveness of the compounds as well as examine their specificity to stabilize ricin A chain. Strikingly, the hit compounds anthothecol, dihydrocelastryl acetate, celestrol, and isogambogic acid appear to target a protein or molecular complex that is common for the destabilization of ER substrates. These compounds likely modulate the function of the proteins involved in the late stages of the degradation process including the proteasome, ubiquitinylation machinery, and general dislocation components. Also, these components could be effective at stabilizing proteins that can cause human diseases such as emphysema or cystic fibrosis.

We have also identified gentian violet and tetrachloroisophthalonitrile as possible compounds that specifically stabilize ricin A chains in the ER. Through the observation of mostly glycosylated, ER-localized ricin A chain and a lack of stability of TCRα chain, the compounds are likely attenuating the dislocation of the ricin A chain by either targeting the ricin molecule itself or by targeting a cellular protein specifically co-opted by ricin toxin to gain access to the cytosol. Collectively, we have demonstrated the proof-of-concept that our assay system is capable of identifying hit compounds specifically for ricin as well as more general dislocation/degradation inhibitors. Collectively, the identified reagents may be utilized for therapeutics for individuals exposed to ricin toxin, other toxins (e.g. shiga and cholera toxin) that utilize a similar cellular pathway, and/or genetic diseases induced by the instability of a mutant ER protein. Our future experiments plan to screen additional chemical compounds to identify the most effective anti-ricin compounds and perform secondary assays that examine a compound's effectiveness in cells and an animal model.

REFERENCES:

1. **Allen, S. C., K. A. Moore, C. J. Marsden, V. Fulop, K. G. Moffat, J. M. Lord, G. Ladds, and L. M. Roberts.** 2007. The isolation and characterization of temperature-dependent ricin A chain molecules in Saccharomyces cerevisiae. FEBS J **274:**5586-5599.
2. **Aridor, M.** 2007. Visiting the ER: the endoplasmic reticulum as a target for therapeutics in traffic related diseases. Adv Drug Deliv Rev **59:**759-781.
3. **Aridor, M., and L. A. Hannan.** 2002. Traffic jams II: an update of diseases of intracellular transport. Traffic **3:**781-790.
4. **Endo, Y., and K. Tsurugi.** 1987. RNA N-glycosidase activity of ricin A-chain. Mechanism of action of the toxic lectin ricin on eukaryotic ribosomes. Journal of Biological Chemistry **262:**8128-8130.
5. **Fiebiger, E., C. Hirsch, J. M. Vyas, E. Gordon, H. L. Ploegh, and D. Tortorella.** 2004. Dissection of the dislocation pathway for type I membrane proteins with a new small molecule inhibitor, eeyarestatin. Mol Biol Cell **15:**1635-1646.
6. **Frankel, A., D. Schlossman, P. Welsh, A. Hertler, D. Withers, and S. Johnston.** 1989. Selection and characterization of ricin toxin A-chain mutations in Saccharomyces cerevisiae. Mol Cell Biol **9:**415-420.
7. **Hampton, R., D. Dimster-Denk, and J. Rine.** 1996. The biology of HMG-CoA reductase: the pros of contra-regulation. Trends Biochem Sci **21:**140-145.
8. **Hirsch, C., D. Blom, and H. L. Ploegh.** 2003. A role for N-glycanase in the cytosolic turnover of glycoproteins. Embo J **22:**1036-1046.

9. **Hosomi, A., K. Tanabe, H. Hirayama, I. Kim, H. Rao, and T. Suzuki.** 2010. Identification of an Htm1 (EDEM)-dependent, Mns1-independent Endoplasmic Reticulum-associated Degradation (ERAD) pathway in Saccharomyces cerevisiae: application of a novel assay for glycoprotein ERAD. The Journal of biological chemistry **285:**24324-24334.
10. **Huppa, J. B., and H. L. Ploegh.** 1997. The alpha chain of the T cell antigen receptor is degraded in the cytosol. Immunity **7:**113-122.
11. **Kim, I., J. Ahn, C. Liu, K. Tanabe, J. Apodaca, T. Suzuki, and H. Rao.** 2006. The Png1-Rad23 complex regulates glycoprotein turnover. The Journal of cell biology **172:**211-219.
12. **Li, S., R. A. Spooner, S. C. Allen, C. P. Guise, G. Ladds, T. Schnoder, M. J. Schmitt, J. M. Lord, and L. M. Roberts.** 2010. Folding-competent and folding-defective forms of ricin A chain have different fates after retrotranslocation from the endoplasmic reticulum. Mol Biol Cell **21:**2543-2554.
13. **Lord, J. M., L. M. Roberts, and W. I. Lencer.** 2005. Entry of protein toxins into mammalian cells by crossing the endoplasmic reticulum membrane: co-opting basic mechanisms of endoplasmic reticulum-associated degradation. Curr Top Microbiol Immunol **300:**149-168.
14. **Lyall, S.** 2003. Arrest of terror suspects in London turns up a deadly toxin, p. 10, New York Times, New York.
15. **Martell, L. A., A. Agrawal, D. A. Ross, and K. M. Muraszko.** 1993. Efficacy of transferrin receptor-targeted immunotoxins in brain tumor cell lines and pediatric brain tumors. Cancer research **53:**1348-1353.
16. **Ng, C. L., K. Oresic, and D. Tortorella.** 2010. TRAM1 is involved in disposal of ER membrane degradation substrates. Experimental cell research **316:**2113-2122.
17. **Nishikawa, S. I., S. W. Fewell, Y. Kato, J. L. Brodsky, and T. Endo.** 2001. Molecular chaperones in the yeast endoplasmic reticulum maintain the solubility of proteins for retrotranslocation and degradation. J Cell Biol **153:**1061-1070.
18. **Noeller, T. P.** 2001. Biological and chemical terrorism: Recognition and management. Cleveland Clinic Journal of Medicine **68:**1001-1016.
19. **Oresic, K., B. Mueller, and D. Tortorella.** 2009. Cln6 mutants associated with neuronal ceroid lipofuscinosis are degraded in a proteasome-dependent manner. Biosci Rep **29:**173-181.
20. **Oresic, K., V. Noriega, L. Andrews, and D. Tortorella.** 2006. A structural determinant of human cytomegalovirus US2 dictates the down-regulation of class I major histocompatibility molecules. The Journal of biological chemistry **281:**19395-19406.
21. **Plemper, R. K., S. Bohmler, J. Bordallo, T. Sommer, and D. H. Wolf.** 1997. Mutant analysis links the translocon and BiP to retrograde protein transport for ER degradation. Nature **388:**891-895.
22. **Rankin, B., C. Boone, and K. Leslie.** 2011. Georgia militia plot: Affidavit outlines plans for killings, The Atlanta Journal, Atlanta.
23. **Redmann, V., K. Oresic, L. L. Tortorella, J. P. Cook, M. Lord, and D. Tortorella.** 2011. Dislocation of ricin toxin A chains in human cells utilizes selective cellular factors. The Journal of biological chemistry **286:**21231-21238.
24. **Reuters.** 2003. France Says Ricin Traces Found in Paris Railway, p. Wire, New York Times, New York.
25. **Sandvig, K., M. L. Torgersen, N. Engedal, T. Skotland, and T. G. Iversen.** 2010. Protein toxins from plants and bacteria: probes for intracellular transport and tools in medicine. FEBS Lett **584:**2626-2634.
26. **Schlossman, D., D. Withers, P. Welsh, A. Alexander, J. Robertus, and A. Frankel.** 1989. Role of glutamic acid 177 of the ricin toxin A chain in enzymatic inactivation of ribosomes. Mol Cell Biol **9:**5012-5021.
27. **Slominska-Wojewodzka, M., T. F. Gregers, S. Walchli, and K. Sandvig.** 2006. EDEM is involved in retrotranslocation of ricin from the endoplasmic reticulum to the cytosol. Mol Biol Cell **17:**1664-1675.
28. **Wesche, J., A. Rapak, and S. Olsnes.** 1999. Dependence of ricin toxicity on translocation of the toxin A-chain from the endoplasmic reticulum to the cytosol. J Biol Chem **274:**34443-34449.

29. **Wiertz, E. J., T. R. Jones, L. Sun, M. Bogyo, H. J. Geuze, and H. L. Ploegh.** 1996b. The human cytomegalovirus US11 gene product dislocates MHC class I heavy chains from the endoplasmic reticulum to the cytosol. Cell **84:**769-779.
30. **Wiertz, E. J., D. Tortorella, M. Bogyo, J. Yu, W. Mothes, T. R. Jones, T. A. Rapoport, and H. L. Ploegh.** 1996. Sec61-mediated transfer of a membrane protein from the endoplasmic reticulum to the proteasome for destruction. Nature **384:**432-438.
31. **Worth, R. F.** 2004. Ricin on Capitol Hill: Connecticut; Suspicious Powder Found at a 2nd Location, p. 19, New York Times, New York.

APPENDICES: NONE